

Motion Capture-driven Musculoskeletal Spine Modeling: An OpenSim-based Inverse Kinematics Approach

Lukas E. P. CONNOLLY^{1,2,3}, Stefan SCHMID^{4,*}, Greta MOSCHINI^{3,5,6},
Michael L. MEIER^{1,2}, Marco SENTELER^{3,5,6}

¹Integrative Spinal Research, Department of Chiropractic Medicine, Balgrist University Hospital, University of Zürich, Zurich, Switzerland; ²University of Zurich, Zurich, Switzerland; ³Department of Health Science and Technology, ETH Zurich, Zurich, Switzerland; ⁴Spinal Movement Biomechanics Group, Division of Physiotherapy, Department of Health Professions, Bern University of Applied Sciences, Bern, Switzerland; ⁵Department of Orthopedics, Balgrist University Hospital, University of Zurich, Zurich, Switzerland; ⁶Institute for Biomechanics, ETH Zurich, Zurich, Switzerland

Corresponding author:

*Stefan Schmid, PT, PhD, Bern University of Applied Sciences, Department of Health Professions,
Murtenstrasse 10, 3008 Bern, Switzerland, +41 79 936 74 79, stefanschmid79@gmail.com

ABSTRACT

Mechanical loads on the human spine play a crucial role in the etiology of disorders of the lower back. In vivo evaluations are complex and highly invasive, therefore musculoskeletal biomechanical models are used to estimate muscle forces and spinal loads during static and dynamic activities. Subject-specific models instead of generic models have the potential to improve diagnosis and optimize clinical treatment by predicting accurate outcomes on an individual basis.

In this study, we developed a method to model a personalized sagittal spinal alignment based on the external back profile obtained from motion capture (MoCap) data to improve the estimation of spinal kinematics and intervertebral joint loading. The spinal alignment adjustments proposed in this study were applied to a full-body generic musculoskeletal model, combined from a well-validated model for the thoracolumbar spine and a model of the lower extremities, to allow simulating predominant activities of daily living. This novel method predicts intervertebral joint centers with an average mean error of 0.99 ± 0.68 cm in the frontal axis and 1.21 ± 0.97 cm in the transverse axis relative to radiographic reference data. The maximum mean joint prediction errors are 1.34 ± 0.73 cm in the frontal axis (T1/T2 joint) and 1.65 ± 1.11 cm in the transverse axis (T3/T4 joint). The generated subject-specific models in this study were able to reproduce spine kinematics and dynamics for each subject and derive qualitative joint load predictions with high task repeatability. The results of this study demonstrate the suitability of the proposed method and associated OpenSim workflow for inter- and intra-subject investigations of muscle activity and joint reaction forces in the spine.

Keywords: Subject-specific; full-body; spinal curvature; functional activities; EOS

1. INTRODUCTION

Musculoskeletal models and computer simulations play an increasingly important role in solving complex dynamic problems and have great potential to improve diagnosis and treatment of musculoskeletal disorders. They allow the estimation of muscle activities and joint reaction forces, which are difficult to measure experimentally (Bassani et al., 2018). In this context, software tools developed for musculoskeletal modeling have facilitated the expansion of clinical applications (Damsgaard et al., 2006, Valente et al., 2017). The open-source platform OpenSim (Delp et al., 2007) is frequently used as a reference for spine modeling and related biomechanical studies (Senteler et al., 2014, Schmid et al., 2020, Kim et al., 2017).

One of the main challenges in musculoskeletal modeling is creating a general model that can replicate various tasks and solve dynamic simulations without requiring task-specific modifications such as described, for example, by Beauchage-Gavreau et al. (2019). Multibody models developed in OpenSim are usually driven using skin marker-based three-dimensional (3D) motion capturing (MoCap), an accurate and reliable method to record human movement. Besides calculating joint angles with an inverse kinematic approach, marker trajectories are used for scaling generic musculoskeletal models to adapt them for subject-specific geometry. This scaling procedure introduces several errors, as it does not currently account for subject specific anatomical differences, especially in the spinal region. The spine is a multi-joint complex consisting of 24 vertebral bodies, each of which has its own dimension and anatomical arrangement, resulting in distinctive sagittal spinal alignments.

The objectives of this study are to develop a robust modeling approach for assessing spinal kinematics and forces acting on the spine for various functional activities. The method shall enable intra-subject or inter-subject investigations of muscle activity and joint reaction forces as, for example, required to investigate loading characteristics of low back pain subjects and compare them to healthy controls. The novel approach should improve subject-specific scaling and simulation accuracy, by modifying the spinal curvature of a generic OpenSim model to create a subject-specific alignment based on the external back profile defined by skin superficial markers. As a result, the personalized spine modeling approach should reduce joint angle estimation errors associated with inverse kinematics, guaranteeing a reliable virtual reproduction of the 3D motion collected in the laboratory.

2. MATERIALS AND METHODS

2.1. Base models

OpenSim-based female and male full-body models were used as a basis for creating the subject-specific models. These base models were composed from a fully articulated thoracolumbar spine model with a head-neck-complex as well as upper extremities (Bruno et al., 2015, Bruno et al., 2017) and the Gait2354 model (Anderson and Pandy, 2001; Carhart, 2000; Delp et al., 1990; Yamaguchi and Zajac, 1989), a standard lower body model available in OpenSim. The models were scaled and combined as described by Schmid et al. (2015). To reduce complexity of the model and improve simulation robustness, external and internal intercostal muscle groups were removed from the model and ribs were considered as rigid bodies attached to the vertebrae. The axial rotation (AR) and lateral bending (LB) coordinates of the thoracic intervertebral joints (IVJ) were locked (T1/T2-T11/T12) thereby reducing the thoracic joints to pin joints with one degree of freedom (flexion and extension (FE)). Additionally, the translational coordinates of the rib to sternum joints were locked, changing the joints' behavior from free to ball joint. To supplement the muscles (i.e., to account for synergistic passive structures such as the thoracolumbar fascia) and prevent model failure in tasks demanding a large range of motion (e.g., lifting a box or standing up from a chair) or

high impact forces (e.g., running), coordinate actuators were added to some joints with infinite minimum and maximal control values. The FE, AR and LB coordinates of the L3/L4 to L5/S1 intervertebral joints were actuated with an optimal force of 10 Nm, whereas the remaining lumbar IVJ were actuated with an optimal force of 5 Nm (T12/L1 to L2/L3). For the thoracic IVJ, only the FE coordinate was actuated with an optimal force of 1 Nm. To further improve simulation robustness, the coordinate actuators of the sternum (SternumRotX, SternumRotY and SternumRotZ), the hip (hip_flexion, hip_adduction and hip_rotation), the knee (knee_angle), and the ankle (ankle_angle) were all actuated with an optimal force of 25 Nm. To compensate for the dynamic inconsistency between the estimated model accelerations and the measured ground reaction forces, residual actuators were added to all six degrees of freedom (i.e., Fx, Fy, Fz, Mx, My, Mz) of the “pelvis_ground” joint, which connects the model freely to the ground (origin of the coordinate system).

Virtual markers were added to the model to allow an inverse kinematics approach driven by motion-capture data from a movement laboratory. For this study, the full-body marker set described by Schmid et al. (2017) was chosen, for its demonstrated capacity in the assessment of spine kinematics during various functional activities (Suter et al., 2020). The markers were placed with the drag and drop OpenSim graphical user interface, for bilateral markers (such as Right Forehead (RFHD) and Left Forehead (LFHD) etc.) the locations were mirrored to create a symmetric virtual marker set, as can be seen in Figure 1. To replicate the marker set on the opposite gender model, the marker offset to the linked body segment was scaled with the same scaling factor as the linked body segment was scaled previously. The base models created for this study can be found in the supplementary material.

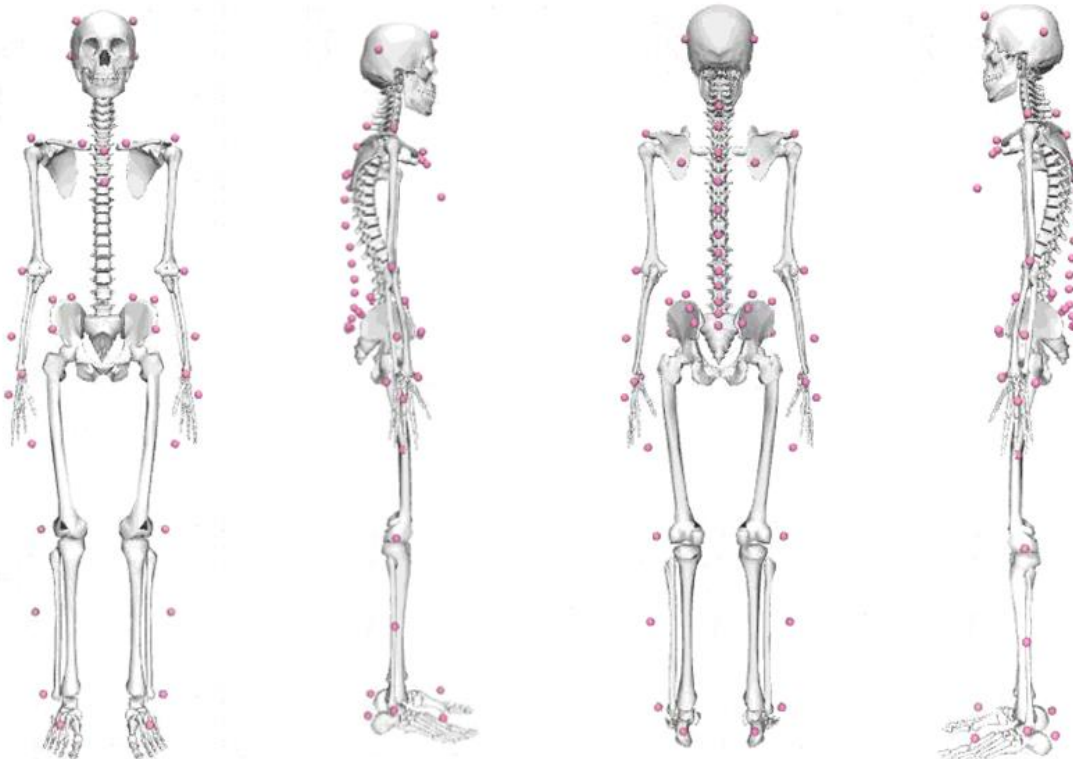


Figure 1: The generic male full-body model enhanced with 58 virtual markers according to the configuration described by Schmid et al. (2017).

2.2. Subject-specific models

To create a subject specific model, we selected the base model according to the gender of the subject and then scaled the model using the OpenSim scaling tool. This tool scales all segments by factors obtained from the distances between experimental markers in the static standing trial (see Table 1). Following the resizing of segments, the mass properties of the body segments were scaled to preserve mass distribution and reproduce the total mass of the subject (recorded using a standard scale). Muscle properties, such as fiber length and tendon slack length were scaled proportionally to the total muscle resting length. Additionally, virtual marker locations were adapted to precisely match the experimental markers by using the OpenSim scaling tool option ‘*Adjust Model Markers*’.

Table 1: Scaling of bodies using measurements based on reference marker pairs (marker names in brackets, according to full boy marker set by Schmid et al., 2017).

Measurement Name	Reference Marker Pairs	Scaled Bodies (X, Y, Z)
Torso	C7 → SACR (S2)	Pelvis, Sacrum, Abdomen, all Intervertebral Bodies, all Ribs, Sternum, Clavicles, Scapularies, Head / Neck
Upper Extremities	(R/L)SHO → (R/L)FIN	Humerus, Ulna, Radius, Hand (all bilateral)
Lower Extremities	(R/L)ASI → (R/L)ANK (R/L)THI → (R/L)ANK	Femur, Tibia, Talus, Calcaneus, Toes (all bilateral)

Subsequently, spinal curvature was adjusted in MATLAB (MathWorks, Inc., Natick, MA, USA) using the external back profile derived from fitting a 4th order polynomial through the sagittal plane coordinates of the markers placed over the spinous processes of C7, T3, T5, T7, T9, T11, L1-L5 and the sacrum (approximately height of S2) (Figure 2A). Input points for the internal spinal curvature polynomial were acquired by subtracting the scaled marker to joint center distance (in the base model) from the smoothed marker position. Underlying assumption was a vertebral orientation along the normal vector of the external back profile polynomial at the height of the corresponding experimental marker (Figure 2B). An exception was the predicted joint center point for C7/T1 and T1/T2, the reason being that the “head_neck” segment, to which the C7 marker is linked to, is always oriented horizontal to the ground coordinate system in the base model. Therefore, the T1/T2 joint location offset to the C7 marker was used as argument to calculate the T1/T2 predicted joint center.

The sagittal plane projection of the geometric center between the two posterior head markers (RBHD and LBHD) was added as a supporting point to better account for cervical lordosis. These points were then used to fit a second 4th order polynomial to predict the internal spinal curvature (Figure 2C) and the estimated joint center locations in the sagittal plane derived from the polynomial by setting the vertical height of each IVJ in the scaled base model as function input (Figure 2D). The orientation of each vertebrae was derived from the angle of the normal vector at the joint center with respect to the frontal axis (Figure 2E). Subject-specific spinopelvic alignment was not considered and therefore, the sacrum and pelvis inclination of each personalized model was kept equal to the base model.

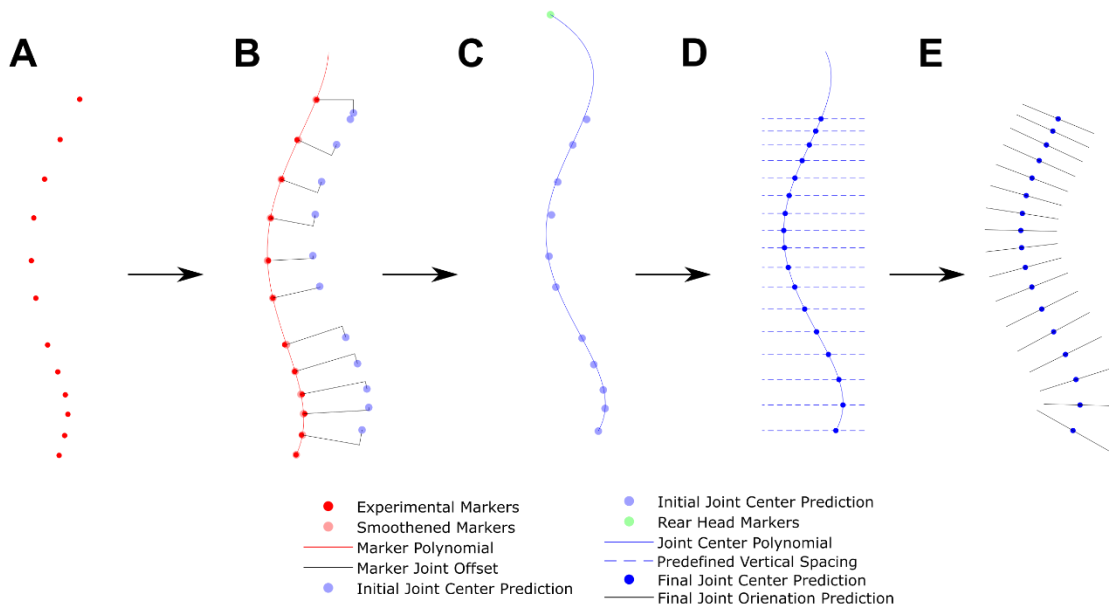


Figure 2: A) Experimental spinal markers attached to the vertebral processes on the skin. B) Approximation of intervertebral joint centers obtained by subtraction of the scaled OpenSim joint center to marker offsets oriented with the normal vector of the external back profile (4th order polynomial). C) Calculated internal spine shape using rough joint center prediction points and supporting posterior head marker center point obtained from the 4th order polynomial. D) Predicted final joint center with predefined (generic model) relative vertical distances between intervertebral joints and internal spine shape. E) Calculated final joint orientation with the normal vector to the internal spine polynomial.

Estimated joint locations and orientations were converted from global to local three-dimensional coordinate systems. The joint coordinate systems of the template model coincided with the centroid of the corresponding vertebral bodies. Thus, location and orientation of each joint center was calculated with respect to the former joint in a global frame and converted to a local coordinate system by fixing each joint center in space and rotating the reference frame by its orientation angle. Additional model modifications such as ribs and sternum reorientation and relocation were made to maintain the global distance and orientation from the base model to the modified spine. Center of mass locations for each spinal segment were readjusted to ensure the same relative position to the vertebral body. Muscle fiber and tendon slack length were adjusted to match the proportions of the base model.

2.3. Validation Studies

2.3.1 Adjustment of spinal alignment

To validate the adjustment of spinal alignment, we conducted a radiographic analysis with three subjects (2 females / 1 male, age: 27 ± 7.5 y, weight: 64.3 ± 13.7 kg, height: 173.7 ± 5.7 cm) of the sagittal plane back profile using radio-opaque skin markers that were placed over the spinous processes of C7, T3, T5, T7, T9, T11, L1-L5 and the sacrum as described above (Figure 1). Radio-opaque metallic spheres (fiducial) with a diameter of 3.5mm were inserted into standard retro-reflective skin markers with identical dimensions and properties as the markers used in the motion analysis laboratory. Once the modified markers were positioned

on the subject, the subject underwent a full body biplanar radiographic examination in the upright standing position using a low dose clinical x-ray scanner (EOS; EOS Imaging, Paris, France). From the lateral radiographs, the centers of all vertebral bodies (ground truth) were calculated as the average position of the four annotated corner points in the sagittal plane using a custom graphical user interface developed in MATLAB (MathWorks, Inc., Natick, MA, USA). Subsequently, a modeled internal spinal curvature was predicted using the marker positions from the radiograph as input. To estimate the accuracy of the spinal curvature modeling method, we calculated the difference between ground truth and the predicted joint centers for all three subjects, as well as the mean errors between subjects in terms of position (frontal and transverse axis), vertebrae orientation and the two most-used spinopelvic parameters: lumbar lordosis (LL) and thoracic kyphosis (TK) angles.

2.3.2 Simulation of spinal loading during various functional activities

To ensure the suitability of our subject-specific models for simulating spinal loading during various functional activities, we recruited seventeen healthy subjects (13 males / 4 females, age: 28 ± 4.95 y, weight: 76.6 ± 10.4 kg, height: 179.3 ± 7.84 cm) with no history of chronic back pain and no episodes of back pain within the last three months and invited them for a single visit to the movement laboratory at the Balgrist University Hospital in Zurich, Switzerland. After the acquisition of relevant anthropometric data, subjects were equipped with retro-reflective markers in a configuration corresponding to the one implemented in the model (see Figure 1) and asked to stand upright for 10s as well as to perform various functional activities such as walking, running, lifting a 5kg box, standing up from a chair and climbing stairs. Dynamic tasks were repeated five times. Motion data were recorded at a sampling rate of 200 Hz using a 27-camera optical motion capture system (Vicon, Oxford, UK). Recorded data were processed using the software Nexus (Vicon, Oxford, UK) and transformed into the OpenSim reference system by implementation of a custom MATLAB script. Ground reaction forces were recorded at a sampling rate of 1 kHz using six level ground embedded force plates (AMTI, BP400600) and two mobile force plates (Kistler, 9260AA6) mounted on the first and second step of a four-step staircase.

Following data acquisition, subject-specific models were generated with the mean marker locations obtained during the first five seconds of the upright standing trial. For the box lifting task, a separate set of models was created by adding 2.5 kg to each hand and updating the inertial properties to account for the measures of the respective side of the box. No other model properties were changed for the box lifting task. Start- and end-events for walking, running and stair climbing tasks were set manually with the software Nexus based on visual inspection of the marker trajectories. Walking and stair climbing start events were set when the right foot left the ground after the left foot had activated the first force plate and end events were set just before the left foot strikes on the third step / force plate. To account for different running speeds, which the subjects were free to choose, the simulations included only the flight phases and stance phase of the left foot on one single force plate, therefore the start event was selected after foot off by the right foot and ended before the right foot strike event. For the standing up from a chair and lifting a box tasks, a custom MATLAB script selected start- and end-events by computationally analyzing the marker trajectories. The box lifting task used the C7 marker as reference. The start event was defined after the vertical marker velocity exceeded 5% of the maximal measured vertical velocity for the first time and ended when the velocity fell below the 5% threshold. Events for standing up from a chair used the STERNUM marker as reference trajectory. Start events were defined when the horizontal velocity exceeded 5% of the maximal horizontal velocity for the first time and end events were set when the vertical velocity fell below 5% of the maximal vertical velocity after reaching peak vertical velocity.

The simulation of spinal loading using the subject-specific models was carried out in three steps: 1. Inverse kinematic analysis to obtain joint angles at each timepoint, by solving a weighted least squares error problem. Marker weights for the ankles (RTOE, LTOE, RANK, LANK, RHEE and LHEE), the knees (RKNE, LKNE), the elbows (RELB, LELB), and the fingers (RFIN, LFIN) were set at 10. All other markers were assigned a weight of one, as they either had a high risk for soft tissue artifacts and / or had many adjacent markers. 2. The kinematic parameters, together with ground reaction forces, were used as input for performing static optimization to estimate muscle activity and force by minimizing the sum of squared muscle activations (Crowninshield and Brand et al., 1981). 3. Joint reaction forces (joint reaction analysis) were then computed by solving the static equations for each timepoint and joint using the estimated muscle forces from static optimization, the experimental ground reaction forces, and the segmental masses.

To validate the predicted joint reaction forces quantitatively, we compared our compressive joint reaction force estimations at the level of L1/L2 (means of all seventeen subjects) with the L2 instrumented vertebral body replacement (VBR) measurements from the OrthoLoad database (<https://orthoload.com>) for lifting a box, standing up from a chair, stair climbing and level walking. Only measurements with comparable conditions as defined in this study were used for comparison, hence measurements with a different type of chair or lifting a different kind of object were excluded. Nonetheless, not all conditions could be matched. For lifting the closest match were measurements of subjects lifting a box with 6 bottles and a weight of 7 kg. For walking and stair climbing the subjects wore slippers or shoes. Running was not compared as measurements were done on a treadmill with a speed of 5 or 6 km/h only and consequently did not contain any flight phases between stance phases.

3. RESULTS

3.1. Spinal alignment

The method estimated lumbar joint centers with an absolute average mean error of 0.99 ± 0.68 cm in the frontal axis and 1.21 ± 0.97 cm in the transverse axis (Figure 3 & 4). The maximum mean joint prediction errors were 1.34 ± 0.73 cm in the frontal axis (T1/T2 joint) and 1.65 ± 1.11 cm in the transverse axis (T3/T4 joint). The mean prediction orientation error for the vertebral bodies in the sagittal plane was $4.74^\circ \pm 2.78^\circ$. The maximum mean error was calculated at the joint level of T10/T11 with $8.68^\circ \pm 1.47^\circ$. Although the errors in the lower thoracic region were relatively large, the standard deviations were small, indicating systematic errors in this region. The standard deviation at the L5/S1 level was comparably large with 3.42° . Although the average mean absolute error was $7.56^\circ \pm 5.30^\circ$ for the prediction of lumbar lordosis, signed errors varied from $+14.28^\circ$ to -7.10° , indicating that this prediction error is a consequence of the large variation of prediction errors at L5/S1. For thoracic kyphosis, the average mean absolute error is $7.26^\circ \pm 3.41^\circ$. The signed prediction errors range from $+11.98^\circ$ to $+4.02^\circ$, hence it seems that the method systematically overpredicts thoracic kyphosis angles.

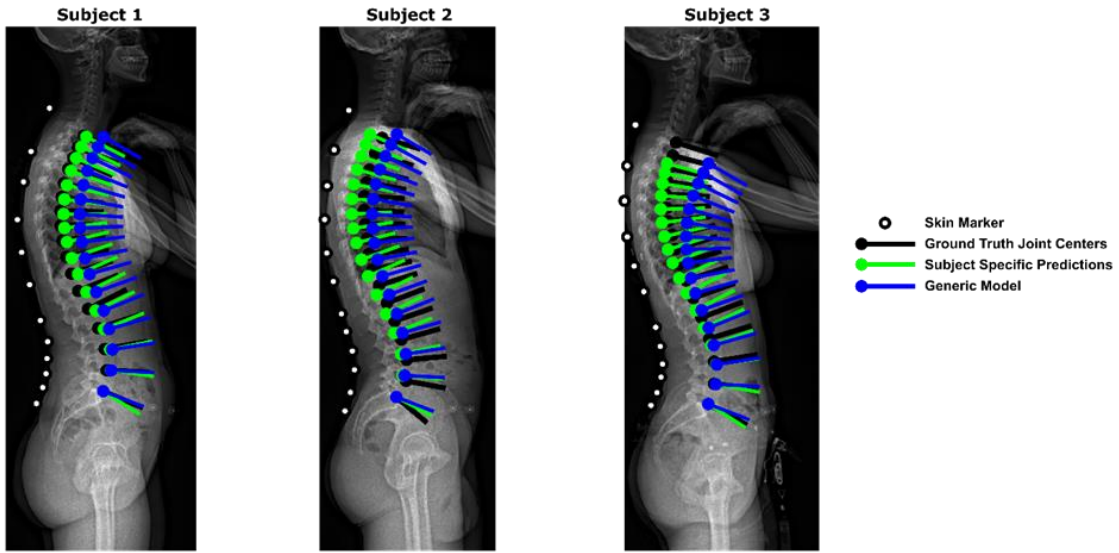


Figure 3: Subjects with ground truth (black), subject specific (blue) and generic (green) joint locations and orientations.

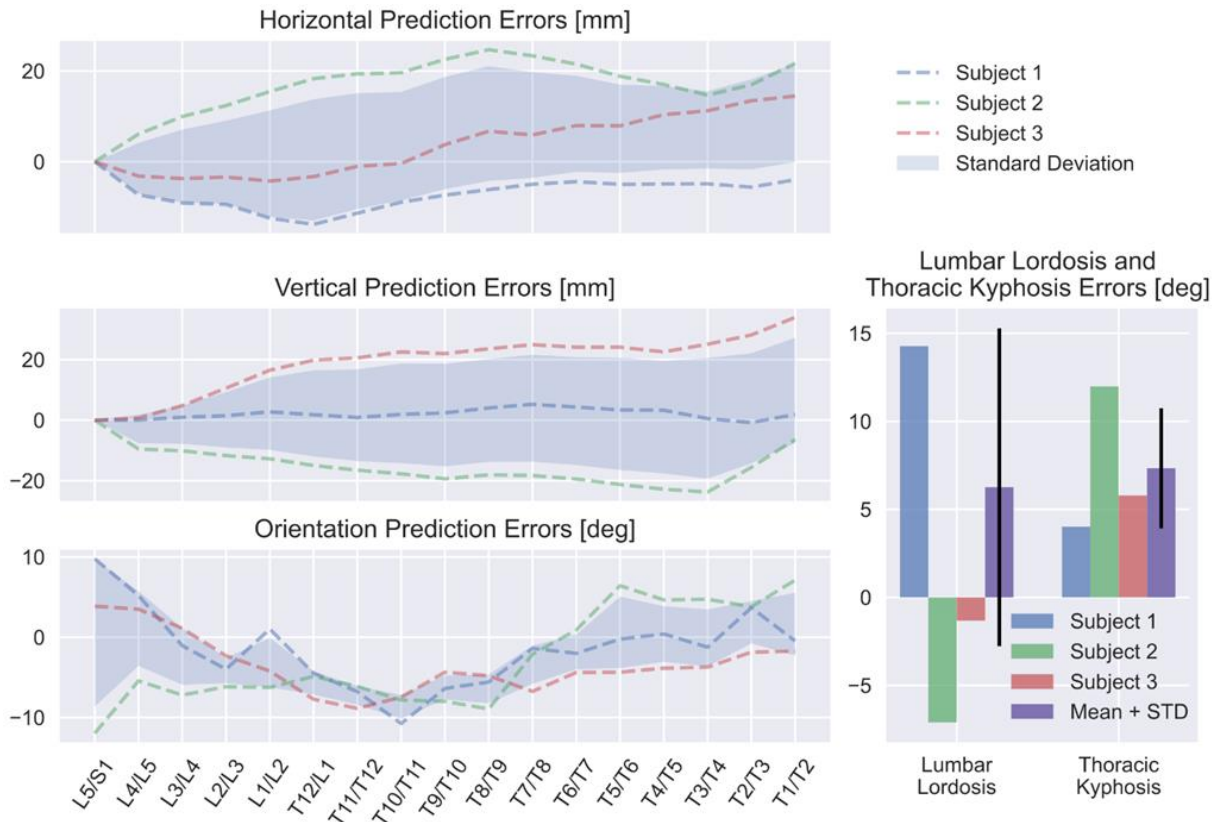


Figure 4: Joint center and spinal curvature prediction errors for all three subjects.

3.2. Spinal loading simulations

Subject-specific spinal alignment models were created and used to simulate different functional tasks using kinematic data collected in the laboratory. Compressive joint reaction loads were calculated on all lumbar IVJ for all the different types of activities recorded experimentally for all subjects (Figure 5). The upper body model of Bruno et al., 2015 and

2017, including coordinate actuators, was sufficiently strong to satisfy equilibrium during static optimization for gait, running, sit-to-stand, stair climbing and lifting a box. As expected, the lowest compressive loads are expressed during level walking, with a peak load of ~ 15 N/kg. They increase in running, and during lifting they rise about three times higher than for level walking.

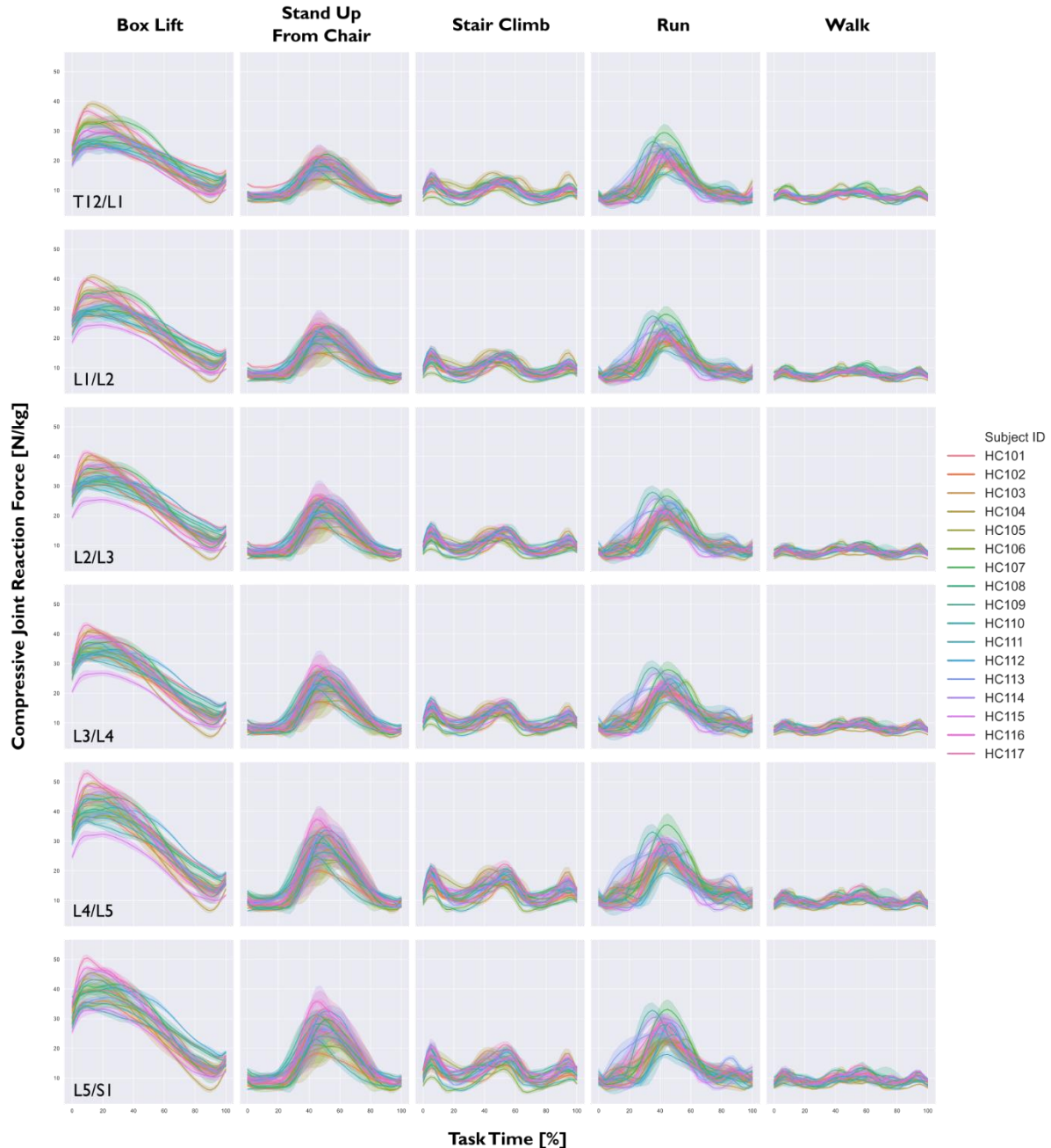


Figure 5: Compressive joint loads for all subjects, lumbar joints (L5/S1 to T12/L1) and different functional tasks. The standard deviation for the five repetitions is shown by the shaded area around each curve.

Reproducibility of the tasks on an inter- and intra-subject level was verified qualitatively by comparing the load curves in Figure 5 with each other. Load curves of all seventeen subjects showed similar shapes for all tasks. Largest observable differences were found for running, where running techniques such as forefoot and heel strike running seemed to cause differently

shaped load curves. On the intra-subject perspective, the standard deviations (shaded area around curves) were small compared to the absolute load values.

The comparison of the calculated compressive joint loads for the generic- and subject-specific models demonstrated that the shape of the load curves was not changed by the custom spine alignment. On the other hand, the magnitudes of the joint loads of the subject-specific model were either the same, lower, or greater compared to the generic model (Figure 6).

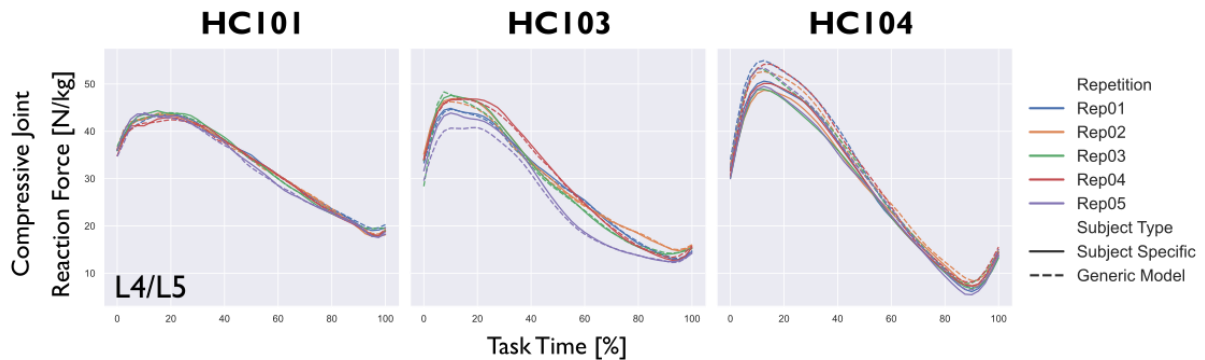


Figure 6: Exemplary subject-specific compressive joint loads obtained by musculoskeletal simulations for lifting task of three subjects at L4/L5 level. They were either close to equal (left), larger (center), or lower (right) compared to the generic model.

The comparison of the study's results and the orthoload measurements showed similar trends for both the OpenSim models and the in vivo measurements (Figure 7), suggesting that the inverse kinematic and static optimization approach accurately predicted joint loads. However, the predicted values were larger than the in vivo acquired data.

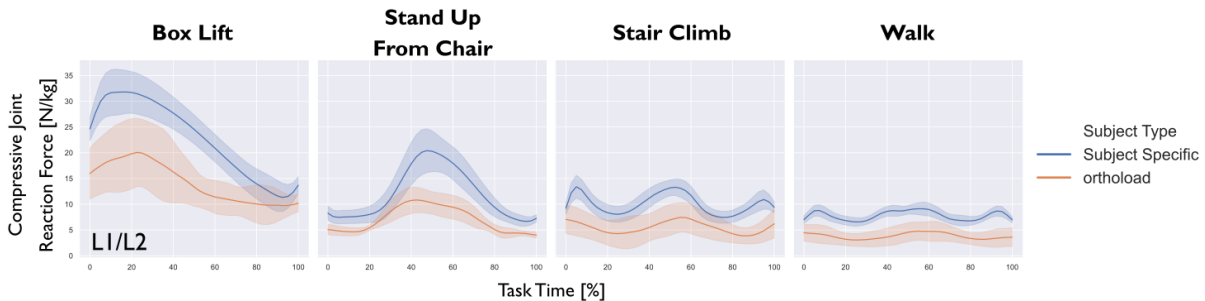


Figure 7: Compressive joint loads for L1/L2 of the subject-specific OpenSim model (blue) compared to in vivo measurements of an L2 VBR from the OrthoLoad database (orange).

4. DISCUSSION

The objective of this study was to develop a robust full-body model to assess spine kinematics and kinetics for a variety of functional activities. This objective was achieved by combining two previously validated OpenSim models and reducing the complexity of the combined model by introducing new constraints and by adding actuators. A novel method of accounting for subject-specificity was introduced by adjusting spinal curvature after standard inbuilt OpenSim model scaling.

We used the external back profile defined by marker locations in upright standing posture to predict joint centers (Figure 2) and design a personalized OpenSim model with fully

articulated spine. There are several advantages to this method: it does not require radiation exposure, it is non-invasive and timesaving, as it only relies on static posture, recorded by a default trial in each MoCap acquisition. The comparison of the ground truth model, the subject specific spinal alignment model, and the generic OpenSim model created for the radiographic validation study showed that the joint center prediction is significantly improved when using the presented method.

A challenge for this study was to create a general model that can replicate and solve activities which require a large range of motion. Most of the models published in literature have been validated for one or two tasks (Raabe et al., 2016, Beaucage et al., 2019) that usually did not implicate large trunk inclination ($> 50^\circ$ angle of flexion). In contrast, our model was able to solve subject-specific joint reaction force estimations for level walking, running, rising from a chair, lifting a 5 kg box and stair climbing using subject-specific kinematic data. We demonstrated that the intra-subject variability measured by our model for repetitions of a task was minimal (Figure 5), but that there are inter-subject differences in loading curves, indicating that the simulation pipeline and the reference model are robust. Therefore, the entire workflow represents a powerful tool to answer specific research questions as well as for clinical applications.

The study has some limitations that should be addressed. The radiographic validation of the method was only done with three subjects, which is not sufficient to conclusively evaluate this method. The upright standing posture in the EOS (arms lifted in front of torso) was also slightly different from the calibration static standing trial in the movement lab (arms hanging on the side). There might be differences in the spinal alignment for these two postures, particularly in the upper thoracic segments. Although this issue was previously encountered (Schmid et al., 2015), we were not able to conduct the MoCap and radiographic measurements simultaneously. Our method also relies heavily on the distances between marker and joint center of the base models, which were only set by drag and drop in the OpenSim graphical user interface. Future studies with larger sample sizes should implement linear regression models to better predict distances from skin markers to joint center by variables such as gender, height, weight, and age to increase the subject-specificity of the model and to further improve joint center and vertebral orientation predictions.

Despite the introduction of a subject-specific spinal curvature, the models created with this method remain generic to some extent. To prevent large errors caused by inaccurate marker placements, the method does not adjust the vertical spacing of the vertebrae, which resulted in some significant prediction errors (Figure 3 and Figure 4). The length of the spine is predicted only by the distance between the Sacrum and C7 marker and may lead to scaling errors, as demonstrated by “Subject 3” of the EOS validation study (Figure 3). Using more markers to calculate the scaling factor might improve spinal height approximation, but the prediction of subject-specific vertebral morphometric features, such as disc height, vertebral body height and transverse width will remain a generic input. The center of mass for the trunk segments vary from subject to subject only through the variation in spinal alignment and scaling. For a more subject-specific model, parameters such as individual segmental mass distribution should be included in the model pipeline to improve simulation accuracy.

The robustness of our model comes at the cost of including numerous artificial coordinate actuators in the spine, which support movements that the optimizer cannot find solutions for when using only the modeled muscles. The necessity for this strategy is that the model does not account for the mechanical properties of non-muscular soft tissue (e.g., spinal ligaments, thoracolumbar fascia, and intervertebral discs) and intra-abdominal pressure. The absence of these model parameters might be an explanation for the quantitative joint load difference observed between the simulation results and the measured *in vivo* data retrieved from the Orthoload database. Other possible explanations for this difference are that the *in vivo* measurements were done with elderly patients after spinal surgery and might therefore not be

directly comparable to a healthy population with an average age of 28 ± 4.95 years. Moreover, the design of the implants (external rods) suggest that the sensors do not account for the entire load transferred through the vertebral body. Hence, the “real” joint loads probably lie somewhere between the *in vivo* measured data and the computationally estimated values from this study.

In conclusion, this study introduces a novel method for creating subject-specific musculoskeletal full-body models based on MoCap data. The approach increases the subject-specificity of the spinal curvature within the model and thereby improves the accuracy of the inverse kinematics approach to assess spinal kinematics. Three-dimensional subject-specific tasks are difficult to simulate, and results need to identify the variability between subject motions and different tasks performed by the same individual. Our novel methodology could achieve both, therefore representing a powerful platform to answer a variety of issues relevant to spinal loading in a scientific and clinical context.

5. CONFLICT OF INTEREST STATEMENT

The authors declare no conflict of interest.

6. ACKNOWLEDGMENTS

This research was supported by the Swiss National Science Foundation (SNF, Bern, Switzerland). Movement analysis was performed with support of the Swiss Center for Clinical Movement Analysis, SCMA, Balgrist Campus AG, Zürich. The authors especially thank Marina Hitz, Linard Filli, and Marc Bolliger from the SCMA for their support.

6. REFERENCES

ANDERSON, Frank C.; PANDY, Marcus G. (2001), Dynamic optimization of human walking. *Journal of Biomechanical Engineering*, 123:5, 381-390.

BASSANI, Tito, GALBUSERA, Fabio (2018). Chapter 15 – Musculoskeletal Modeling. In Galbusera F., Wilke H., editors. *Biomechanics of the Spine: Basic Concepts, Spinal Disorders and Treatments*. 1st ed. Cambridge MA, USA: Academic Press.

BEAUCAGE-GAUVREAU, Erica; ROBERTSON, William S. P.; BRANDON, Scott C. E.; FRASER, Robert; FREEMAN, Brian J. C.; GRAHAM, Ryan B.; THEWLIS, Dominic; JONES, Claire (2019). Validation of an OpenSim full-body model with detailed lumbar spine for estimating lower lumbar spine loads during symmetric and asymmetric lifting tasks. *Computer Methods in Biomechanics and Biomedical Engineering*, 22:5, 451-464.

BRUNO, Alexander G.; BOUXSEIN, Mary L.; ANDERSON, Dennis E. (2015). Development and validation of a musculoskeletal model of the fully articulated thoracolumbar spine and rib cage. *Journal of biomechanical engineering*, 137:8: 081003.

BRUNO, Alexander G.; BURKHART, Katelyn; ALLAIRE, Brett; ANDERSON, Dennis E.; BOUXSEIN, Mary L. (2017). Spinal Loading Patterns from Biomechanical Modeling Explain the High Incidence of Vertebral Fractures in the Thoracolumbar Region. *Journal of Bone and Mineral Research*, 32:6: 1282-1290.

CARHART, Michael; YAMAGUCHI, Gary T. (2000) Biomechanical analysis of compensatory stepping: implications for paraplegics standing via functional neuromuscular stimulation [dissertation]. Arizona State University.

CROWNINSHIELD, Roy D.; BRAND, Richard A. (1981). A physiologically based criterion of muscle force prediction in locomotion. *Journal of Biomechanics*, 14:11: 793-801.

DAMSGAARD, Michael; RASMUSSEN, John; CHRISTENSEN, Søren Tørholm; SURMA, Egidijus; DE ZEE, Mark (2006). Analysis of musculoskeletal systems in the AnyBody Modeling System. *Simulation Modelling Practice and Theory*, Volume 14. 8, 1100-1111.

DELP, Scott L.; LOAN, J. P.; HOY, M. G.; ZAJAC, F. E.; TOPP, E. L.; ROSEN, J. M. (1990). An interactive graphics-based model of the lower extremity to study orthopaedic surgical procedures, *IEEE Transactions on Biomedical Engineering*, 37:8, 757-767.

DELP, Scott L.; ANDERSON, Frank C.; ARNOLD, Allison S., LOAN, Peter; HABIB, Ayman; JOHN, Chand T., GUENDELMAN, Eran; THELEN, Darryl G. (2007). OpenSim: open-source software to create and analyze dynamic simulations of movement. *IEEE transactions on biomedical engineering*, 54:11: 1940-1950.

KIM, Hyun-Kyung; ZHANG, Yanxin (2017). Estimation of lumbar spinal loading and trunk muscle forces during asymmetric lifting tasks: application of whole-body musculoskeletal modelling in OpenSim. *Ergonomics*, 60:4: 563-576.

RAABE, Margaret E.; CHAUDHARI, Ajit MW. (2016). An investigation of jogging biomechanics using the full-body lumbar spine model: Model development and validation. *Journal of biomechanics*, 49:7: 1238-1243.

SCHMID, Stefan; STUDER, Daniel; HASLER, Carol-Claudius; ROMKES, Jacqueline; TAYLOR, William R.; BRUNNER, Reinald; LORENZETTI, Silvio; Using Skin Markers for Spinal Curvature Quantification in Main Thoracic Adolescent Idiopathic Scoliosis: An Explorative Radiographic Study. *PLoS ONE*, 2015, 10(8): e0135689. <https://doi.org/10.1371/journal.pone.0135689>.

SCHMID, Stefan; BRUHN, Björn; IGNASIAK, Dominika; ROMKES, Jacqueline; TAYLOR, William R.; FERGUSON, Stephen J.; BRUNNER, Reinald; LORENZETTI, Silvio (2017). Spinal kinematics during gait in healthy individuals across different age groups. *Human Movement Science*, Volume 54, 73-81.

SCHMID, Stefan; BURKHART, Katelyn A.; ALLAIRE, Brett T.; GRINDLE, Daniel; ANDERSON, Dennis E. (2020). Musculoskeletal full-body models including a detailed thoracolumbar spine for children and adolescents aged 6–18 years. *Journal of Biomechanics*, Volume 102, <https://doi.org/10.1016/j.jbiomech.2019.07.049>.

SENTELER, Marco; WEISSE, Bernhard; SNEDEKER, Jess G.; ROTHENFLUH, Dominique A. (2014). Pelvic incidence–lumbar lordosis mismatch results in increased segmental joint loads in the unfused and fused lumbar spine. *European Spine Journal*, 23.7: 1384-1393.

SUTER, Magdalena; EICHELBERGER, Patric; FRANGI, Jana; SIMONET, Edwige; BAUR, Heiner; SCHMID, Stefan (2020). Measuring lumbar back motion during functional activities using a portable strain gauge sensor-based system: A comparative evaluation and reliability study. *Journal of Biomechanics*, Volume 100, <https://doi.org/10.1016/j.jbiomech.2019.109593>.

VALENTE, Giordano; CRIMI, Gianluigi; VANELLA, Nicola; SCHILEO, Enrico; TADDEI, Fulvia (2017). nmsBuilder: Freeware to create subject-specific musculoskeletal models for OpenSim. *Computer Methods and Programs in Biomedicine*, 152: 85-92.

YAMAGUCHI, Gary T.; ZAJAC, Felix E. (1989). A planar model of the knee joint to characterize the knee extensor mechanism. *Journal of Biomechanics*, 22:1, 1-10.